4. The left-right ambiguities are resolved by calculating all 2^6 possible real hit combinations to find which one gives the smallest PCA distance.

5. Finally, a *global* search is performed for the largest set of tracks which both minimizes the sum of the PCA distances and can be removed without incorporating the same hit in two tracks (special provision is, however, taken for unresolved double hits).

6. For each well-identified track segment the following 4 quantities are stored: $(\theta_r,\ \phi_r,\ \theta_p,\ \phi_p)$ where θ and ϕ are the polar and azimuthal angles and the indices r and p denote the position and momentum.

The joining of track segments between tracking stations into a complete track is actually somewhat simpler than finding the segments. The following procedure is used:

1. All possible hit combinations from station #2 and #3 are formed (typically 30×40 candidates in central collisions).

2. A PCA test with $d_{\max} = 4$ is performed to identify reasonable track candidates. Typically 50–200 candidates survive.

3. All track candidates from 2) are combined with track segments from station #1 and a PCA test with $d_{\max} = 3$ is performed to select the final tracks. Since a total of $3 \times 4 = 12$ track segment coordinates enters in this calculation and each track is determined by only 5 parameters, the problem is highly overdetermined and the final PCA test identifies the true tracks extremely efficiently.

Tracking Resolution

PISA simulations of the single track momentum reconstruction were performed with the central and muon magnetic fields turned on, and Landau fluctuations were included in the straggling through the central magnet. A Gaussian distribution of the z-position of the vertex with $\sigma_z = 22$ cm was used.

The acceptance in θ for single muon tracks is $10° < \theta_p < 35°$. The magnetic fields approximately conserve the polar angle, θ, of the tracks, but only to first order. The limits of the θ-acceptance should therefore only be considered approximate. This diffuseness is further enhanced by the multiple scattering in the absorber.

The momentum acceptance is approximately $p > 2.0$ GeV, arising from the minimum muon energy required to penetrate the central magnet coil plus the active thickness of the muon identifier. This 2 GeV limit should also be considered approximate and only detailed simulations can determine if a particular muon track will be identified.

Assuming a position resolution of 0.10 mm for a complete tracking station (corresponding to a resolution of ≈ 0.25 mm per drift chamber) and a vertex position resolution of 0.2 mm, the single track momentum resolution at the vertex was found to be (momentum unit is GeV/c)

$$\sigma(|p|) \quad = \quad \sqrt{0.10^2 + (0.02\ p)^2}$$

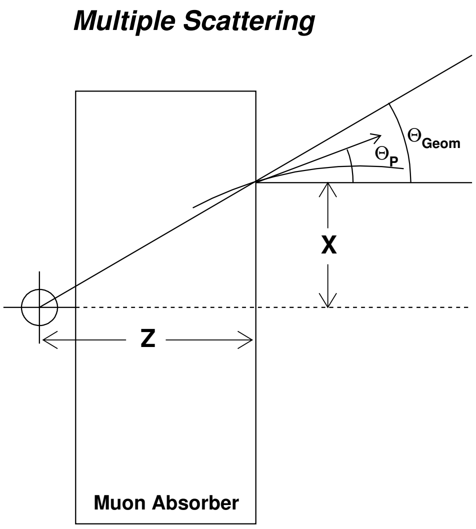

Figure 10.29: Illustration of the relation between the direction of the tangent to the momentum, denoted θ_p, of a particle just exiting the absorber, and the same particle's geometrical direction, denoted θ_{geom}, given by the position at which it exits combined with a precise knowledge of the interaction vertex. The curved track represents the particle's trajectory.

$$\begin{aligned} \sigma(\theta_p) &= 0.5^\circ \\ \sigma(\phi_p) &= 2.0^\circ \end{aligned} \tag{10.2}$$

The standard deviations in (10.2) are based on Gaussian fits to the momentum distributions obtained by PISA. At small momenta, the dominant contribution to the resolution is energy- and angle-straggling in the absorber. This contribution is stochastic and therefore difficult to correct. However, by using the difference between the directions of the local momentum vector and the local position vector at the first tracking station, as illustrated schematically in Fig. 10.29, part of this straggling can be estimated. There is a correlation between the quantity $(\theta_{geom} - \theta_p)$ and the actual change in three-momentum due to multiple scattering for a given particle. Determination of the geometric angle, θ_{geom}, requires independent knowledge of the interaction vertex, which is supplied in PHENIX by the silicon vertex detector. This vertex must be known to about 1–2 mm to have the full benefit of this correction proceedure. Applying this correction improves the momentum resolution for small momenta by approximately 50%.

This correction is potentially complicated by the presence of the inner coil of the central magnet inside the acceptance of the muon arm. Particles which traverse this coil and enter the muon arm pass through a variable combination of copper coil, water and insulation, in addition to the pole tip steel and nosecone copper traversed by all primary particles entering the muon arm. The fraction of each material in the flight path of a particle cannot be

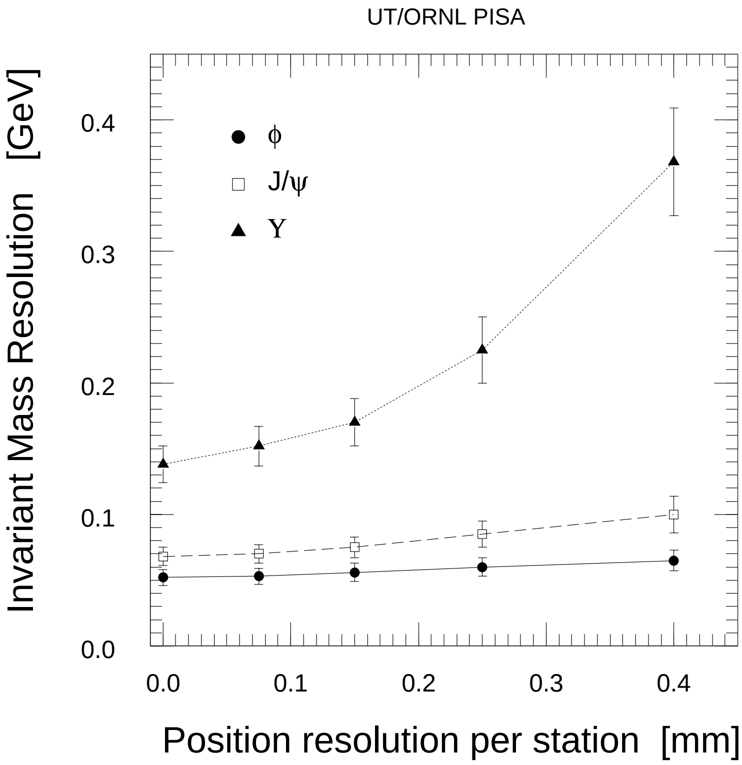

Figure 10.30: Invariant mass resolution of dimuons originating from ϕ, J/ψ and Υ-decay as a function of the position resolution in the spectrometer tracking stations.

determined due to the uncertainty from multiple scattering in the actual trajectory. The specific energy losses in these materials differ, leading to an additional contribution to the energy loss straggling. However, analytic estimates, confirmed by Monte Carlo calculations using PISA, have shown that this term is less than 25% of the main straggling term and thus can be neglected.

Due to the asymmetric nature of Landau fluctuations, the reconstructed momentum distributions generally have a low momentum tail. Consequetly, the standard deviations of the reconstructed momentum distributions are 30–40% larger than the above values from Gaussian fitting. Negative and positive muon tracks can be distinguished with 99% efficiency up to at least 50 GeV/c.

Mass Resolution

As stated earlier, the main purpose of the muon detector is to detect muon pairs originating from vector meson decay or virtual photon production. The most important two-track parameter is the invariant mass resolution, which should be as small as possible to provide

Table 10.4: Single-station tracking efficiency and position resolution as a function of drift chamber occupancy and position resolution. See text for further explanation.

Occupancy	Drift chamber position resolution 100 μm		200 μm		300 μm	
	Eff.	Track res.(μm)	Eff.	Track Res.(μm)	Eff.	Track res. (μm)
2%	99%	45	99%	90	98%	140
4%	99%	45	99%	92	97%	160
6%	99%	46	98%	100	95%	180
8%	98%	48	96%	120	93%	210
10%	97%	53	94%	150	90%	260

a good signal-to-background ratio. The resolution of M_{inv} below 4 GeV/c^2 is dominated by the straggling in the absorber, whereas at higher masses the dominant contribution is the position resolution of the drift chambers. The asymmetric shape of the peaks, with a low energy tail, is caused by Landau fluctuations. The relative mass resolution is approximately given by $\sigma(M)/M = 6\%/\sqrt{M}$; this mass resolution enables a clear separation of ρ and ϕ, J/ψ and ψ', with an acceptable separation of Υ and Υ'.

To specify the drift chamber design criteria, the dependence of the M_{inv} resolution as a function of the position resolution in a complete tracking station was investigated. The calculation shown in Fig. 10.30 was performed with an ORNL/UT algorithm including a correction for straggling, so the absolute values of the M_{inv} resolution differ slightly from the values above. The J/ψ mass resolution is nearly independent of the position resolution, since the dominant contribution here is the straggling in the absorber, whereas the Υ mass resolution varies strongly with the position resolution. Note that Fig. 10.30 shows the position resolution of a complete tracking station, *not* the position resolution of each individual drift chamber. If the position resolution of each of the six individual drift chambers within a tracking station is conservatively assumed to be 0.3 mm, the total tracking station position resolution would be 0.14 mm.

Track Reconstruction Efficiency

Approximately 50, 40, and 35 charged particles pass through the three tracking stations, respectively, for a central Au + Au event. Since the stations have 736, 920, and 1624 channels, respectively, this corresponds to maximum occupancies of 7%, 4%, and 2% (not accounting for particles striking chamber support frames). Most of these particles have low momenta, and only 0.4 particles, on average, penetrate the muon identifier fully. Nevertheless, the spectrometer must track all of the charged particles entering it to measure the momentum of the few muons.

The track finding efficiency of a single tracking station is shown in Table 10.4 as a function of the occupancy and drift chamber position resolution. The efficiency is defined as the ratio

Table 10.5: The overall track reconstruction efficiency of the muon spectrometer for tracks going through all three tracking stations and reaching the muon identifier with a residual momentum of at least 1 GeV/c.

Track Multiplicity	Drift Chamber Position Resolution		
	100 μm	200 μm	300 μm
25	98%	97%	96%
50	96%	94%	91%
75	92%	89%	82%

between the number of completely reconstructed tracks and the number of incident tracks on the station. The position resolution is the standard deviation of the difference between the original and reconstructed track positions in the bend direction. As the occupancy increases, the track reconstruction efficiency decreases, but for all values in the table it stays above 90%. For higher occupancies or worse resolution the efficiency decreases rapidly to unacceptable levels. It is worth noting that most of the missed tracks have large angles of incidence and tend to be strongly bent leakage tracks. The misidentification of high momentum tracks is in general a factor of 2–3 less than the overall misidentification.

A potentially more serious problem than reconstruction inefficiency is the deterioriating resolution caused by misidentification of close hits when the occupancy increases. This creates a tail on the position distribution, which degrades the invariant mass resolution. For drift chamber resolutions at or below 200 μm, and expected occupancy values less than 9%, it does not seem to be a problem, but reduce the efficiencies in Table 10.4 by 2–3%.

The overall reconstruction efficiency for tracks traversing all three tracking stations and reaching the muon identifier with a residual momentum of at least 1 GeV/c is given in Table 10.5 as a function of the track multiplicity and the position resolution. Tracks with reconstructed positions more than five standard deviations from the real position are categorized as lost. The overall track reconstruction efficiency of 90% or better for realistic parameters is very encouraging and demonstrates that the muon detector can handle the high multiplicity environment in high energy nuclear collisions very well.

10.4.3 Muon Identifier

Muon identification is accomplished with a system very similar to the one in the CLEO II detector at the Cornell Electron-positron Storage Ring [7]. The muon identifier will be a calorimeter comprised of three absorbing layers, each of approximately two nuclear absorption lengths thickness, with detectors installed behind each absorber. The muon identifier must separate true muon tracks from the large background of hadrons that punch through the main magnet yoke. The muon identifier built for the CLEO II experiment performs very well; the CLEO II collaboration reports a muon identification efficiency of between 0.89 and 0.99 depending on track penetration requirement with a probability of